The effect of fusidic acid on *Plasmodium falciparum* elongation factor G (EF-G)

Ankit Gupta[1], Snober S. Mir[1], Uzma Saqib[1], Subir Biswas[1], Suniti Vaishya[1], Kumkum Srivastava[2], Mohammad Imran Siddiqi[1], and Saman Habib[1]*

[1]*Division of Molecular and Structural Biology, CSIR-Central Drug Research Institute, Lucknow, India*
[2]*Division of Parasitology, CSIR-Central Drug Research Institute, Lucknow, India*
Running title: Antibiotic sensitivity of *Plasmodium* organelle EF-Gs
**Address for correspondence:* Dr. Saman Habib, Division of Molecular and Structural Biology, CSIR-Central Drug Research Institute, Sector 10, Jankipuram Extension, Sitapur Road, Lucknow-226031, India
Tel: 91-522-2771940 ext. 4977; *Fax*: 91-522-2771941.
E-mail: saman.habib@gmail.com, saman_habib@cdri.res.in

Abstract

Inhibition of growth of the malaria parasite *Plasmodium falciparum* by known translation-inhibitory antibiotics has generated interest in understanding their action on the translation apparatus of the two genome containing organelles of the malaria parasite- the mitochondrion and the relic plastid (apicoplast). We report GTPase activity of recombinant EF-G proteins that are targeted to the organelles and further use these to test the effect of the EF-G inhibitor fusidic acid (FA) on the factor-ribosome interface. Our results monitoring locking of EF-G.GDP onto surrogate *E. coli* ribosomes as well as multi-turnover GTP hydrolysis by the factor indicate that FA has a greater effect on apicoplast EF-G compared to the mitochondrial counterpart. Deletion of a three amino acid (GVG) sequence in the Switch I loop that is conserved in proteins of the mitochondrial EF-G1 family and the *Plasmodium* mitochondrial factor, but is absent in apicoplast EF-G, demonstrated that this motif contributes to differential inhibition of the two EF-Gs by FA. Additionally, the drug thiostrepton, that is known to target the apicoplast and proteasome, enhanced retention of only mitochondrial EF-G on ribosomes providing support for the reported effect of the drug on parasite mitochondrial translation.

Keywords Effect, Fusidic, *Plasmodium Falciparum,* Longation, Factor G (EF-G)

Introduction

The search for new drugs against malaria has focused efforts on identification of new targets in the causal protozoan, *Plasmodium*. Members of the phylum Apicomplexa, which includes *Plasmodium* species, carry a non-photosynthetic plastid called the apicoplast. The organelle is essential for parasite survival and thus pathways operative in the apicoplast as well its housekeeping functions are of interest as sites for drug intervention [1, 2]. Apicoplast pathways may be differentially required in the blood and liver stages of the parasite cycle in the human host and isoprenoid biosynthesis has been demonstrated to be the only apicoplast pathway essential to the parasite in the erythrocytic stages [3]. A single mitochondrion functions in a *Plasmodium* cell and both the apicoplast and mitochondrion adopt extended branched morphologies in blood and liver stages [4, 5].
Housekeeping functions required for apicoplast growth and division have been investigated as targets for antibiotics. Although some apicoplast inhibitors cause a delayed-death effect, their lethal and irreversible effects on apicoplast function and parasite survival makes them plausible

agents of chemotherapy. Inhibition of replication of the 35 kb apicoplast DNA genome by gyrase inhibitory antibiotics ciprofloxacin and novobiocin has potent anti-malarial effects [6, 7]. There is interest in the use of known and novel prokaryotic translation inhibitors that specifically target apicoplast translation [8, 9]. Doxycycline and clindamycin, which target translation in the apicoplast, are already in clinical use. Clindamycin entered advanced clinical trials as a combination drug with fosmidomycin and doxycycline is recommended as a malaria prophylactic for travellers to endemic areas [10, 11]. Point mutations in *Plasmodium falciparum* and *Toxoplasma gondii* apicoplast *rpl4* and *lsu rRNA* genes have been associated with resistance to azithromycin and clindamycin, respectively [12] confirming apicoplast translation as the site of action of these antibiotics. Microbial translation inhibitors have also been shown to block apicoplast development during exo-erythrocytic schizogony in liver stages of *P. berghei*, leading to impaired parasite maturation [13].

All factors required for protein translation in the apicoplast, except apicoplast -encoded elongation factor-Tu (EF-Tu), are encoded by nuclear genes and transported to the organelle. The *Plasmodium* mitochondrion also has a functional translation machinery for synthesis of the three proteins -cytochrome oxidase 1 and III and cytochrome b, encoded by its genome [14] and all translation factors required by the mitochondrion are nuclear-encoded. There is limited information on the localization and function of factors required for organellar translation in *Plasmodium* [15]. Moreover, direct effects of translation-inhibitory antibiotics on target proteins have been rarely investigated in the parasite. Binding of several bacterial EF-Tu targeting antibiotics with apicoplast EF-Tu has also been shown [16] although their effects on activity of the factor remain to be studied. The effect of kirromycin on *in vitro* apicoplast EF-Tu activity has been reported [17]. Johnson et al. [18] have shown that two bacterium-like EF-G proteins, encoded by distinct nuclear genes, are targeted separately to the apicoplast and mitochondrion of *P. falciparum*. Both these are possible targets of the steroid-like antibiotic fusidic acid (FA) which kills blood-stage parasites. FA inhibits protein synthesis in bacteria and acts against many pathogens including *Staphylococcus aureus*, gram-positive anaerobic bacteria, *Neisseria* spp., and *Bordetella pertussis* [19]. It is used clinically as a topical application or systemic treatment, particularly in case of bone and joint infections or skin and soft tissue infections [19].

EF-G has five structural domains (DI to DV). DI is the G (GTPase)-domain, and domain II is common to all translational GTPases [20]. The EF-2 family specific domains DIII-V mimic the structure of aminoacyl-tRNA [21] and bind to the A site of the ribosome. EF-G domains III-V also interact with ribosome recycling factor (RRF) for ribosome disassembly [22]. Mitochondria from yeast to human have been reported to have two EF-G homologs- mtEF-G1 and mtEF-G2. MtEF-G1 mediates translocation while mtEF-G2 functions as a RRF and lacks translocation activity [23, 24]. The spirochaete *Borrelia burgdorferi* has also been reported to contain a second EF-G that functions exclusively as a recycling factor only in the presence of the bacterial RRF [24]. The *P. falciparum* mitochondrion has only one EF-G for mediating translocation [18, 25] and recent results from our laboratory have shown that this EF-G is also required for recycling of ribosomes by the mitochondrion-targeted *Pf*RRF2 [26]. Recycling of apicoplast ribosomes is mediated by an apicoplast targeted EF-G and an apicoplast- specific *Pf*RRF1 [26].

In order to further characterize function of *P. falciparum* organellar EF-Gs and anti-parasitic effects of translation-inhibitory antibiotics targeting the factor, we investigated the effect of FA on recombinant apicoplast and mitochondrial EF-Gs of *P. falciparum*. We report relative resistance of *P. falciparum* mitochondrial EF-G to FA, a property that is at least partly

attributable to the presence of a conserved GVG motif in the switch I loop of all mtEF-G1 proteins; the motif is not found in plastid/apicoplast EF-Gs.

Materials And Methods

2.1. Effect of fusidic acid on *P. falciparum* in vitro culture

SYBR Green assay [27] was performed to detect parasiticidal activity of FA on in vitro blood culture of *P. falciparum* 3D7. Dual synchronized parasites were treated with varying concentrations of FA (Sigma) in ring stages at 0.5% parasitaemia and 1.5% hematocrit. Readings were taken at 48 and 96 hours on Biotek FLX800 instrument (excitation at 485 nm, emission at 530 nm). The use of human RBCs from healthy volunteers for *P. falciparum* culture was approved by the CSIR-CDRI Institutional Ethics Committee (Human Research) (#CDRI/IEC/CEM/21-07-2010). Written informed consent was obtained from voluntary donors for use of this sample in research.

To measure the effect of FA on apicoplast and cytoplasmic translation, synchronized *P. falciparum* 3D7 culture was treated with FA (28 and 93 μM). Parasites were harvested after 28 h by saponin lysis and parasite lysate from equal numbers of parasites was electrophoresed on 10% SDS-PAGE, transferred onto nitrocellulose membrane, and probed with rabbit anti-SufB antibody (1:200 dilution) [28] and mouse anti-tubulin monoclonal antibody (1:1000 dilution) (Sigma). Levels of EF-Tu and tubulin were measured by densitometry.

2.2. Homology modeling and molecular docking

The homology models were constructed using the program MODELLER [29] interfaced with InsightII [30-32]. The homology models of *Pf*EF-G_{Ap} and *Pf*EF-G_{Mit} were derived based on the Y chain of template Elongation Factor G from *Thermus thermophilus* (PDB: 2WRI) [33]. The three dimensional structures obtained were quite superimposable; RMSD (Root Mean Square Deviation) values between the homology models and the template *Tt*EF-G are low (1.390 Å for EF-G_{Ap} and 1.453 Å for EF-G_{Mit}) [34, 35]. In order to assess the overall stereochemical quality of the modeled protein, Ramachandran plot analysis was performed using PROCHECKv3.4.4 [36-38]. PROCHECK results showed only 2.6% and 1.7% residues in disallowed region of the modeled *Pf*EF-G_{Ap} and *Pf*EF-G_{Mit}, respectively; these residues are far from the FA-binding region. The overall structure of the two models came out to be satisfactory.

Docking of FA to the receptor active site was carried out using AUTODOCK 3 [39] which estimates the energy of ligand binding in the receptor binding site. Data on the FA binding site across the *Pf*EF-G_{Ap} and *Pf*EF-G_{Mit} surface was obtained using information from the template used (2WRI). The crystal structure of template *Tt*EF-G (PDB: 2WRI) has bound FA. Considering the conservation of the active site in the *P. falciparum* proteins, the same information was applied to dock FA in the corresponding active sites of EF-G_{Ap} and EF-G_{Mit} using default settings of AUTODOCK3. Docking involved a grid of 101 points in three dimensions with a spacing of 0.375 Å centered on the EF-G models. To assess the docking quality of the AUTODOCK3, the crystal bound FA in the template (2WR1) was redocked onto the same *Tt*EF-G site. The RMSD between the crystal bound and docked FA conformations in the receptor active site was as low as 0.7 Å. The very low RMSD between the original and docked conformations of FA in the receptor active site indicates the excellent performance of the AUTODOCK3 program in terms of accurately predicting the conformation of ligand in the binding site. Further, FA was docked in both *Pf*EF-G_{Ap} and *Pf*EF-G_{Mit} models and the binding energy was determined.

2.3. Recombinant protein expression and purification

*Pf*EF-G_{Ap} (DI-III) (PlasmoDB ID: PF3D7_0602400) was PCR-amplified with parasite genomic DNA as template using the following primers: 5'-CGCGGATCCGTTAATGGTTCAACAAAAAATG-3' (forward) and 5'-CGCGTCGACAGATATCTGAGGTTTCCCATAA-3' (reverse) and cloned into pQE30 (Qiagen). pQE30-EFG_{Ap} (DI-III) was co-transformed into XL1-Blue cells and expression of the 6XHis fusion protein was induced with 0.8 mM IPTG and grown at 20°C for 16 h. His-tagged *Pf*EF-G_{Ap}(DI-III) (~72 kDa) was purified by affinity chromatography through Ni-NTA matrix (MN Biosciences). Purified recombinant *Pf*EF-G_{Ap} (DI-III) was used to generate anti-*Pf*EF-G_{Ap} antibodies in rabbit. Rabbit was immunised with *Pf*EF-G_{Ap} (DI-III) in Complete Freund's Adjuvant followed by two booster doses in Incomplete Freund's Adjuvant. Approval for animal use was given by the Institutional Animal Ethics Committee of the CSIR-Central Drug Research Institute, India (approval no. IAEC/2007/126/Renew) and care of animals was in accordance with Government of India guidelines.

Recombinant *Pf*EF-G_{Ap} (predicted processed form lacking the bipartite apicoplast targeting sequence and containing domains DI-DV) and *Pf*EF-G_{Mit} (PlasmoDB ID: PF3D7_1233000) were cloned, expressed and purified as described in Gupta et al. [26]. The *Pf*EF-G_{Mit}GVG-del mutant was generated using the pGEX-EF-G_{Mit} [26] plasmid as template. PCR primers flanking the GVG motif were used to amplify the plasmid lacking the GVG motif in the switch I region of *Pf*EF-G_{Mit}. The QuickChange XL Site-Directed Mutagenesis Kit (Stratagene) was used for the reaction and the deletion was confirmed by DNA sequencing.

2.4. GTPase assay for EF-G

GTP hydrolysis by recombinant *Pf*EF-G_{Ap} and *Pf*EF-G_{Mit} was measured using the EnzCheck Phosphate Assay Kit (Molecular Probes) as described by Biswas et al. [17]. The effect of fusidic acid (FA) on ribosome-dependent multiple substrate turnover GTP hydrolysis by *Pf*EF-G_{Ap} and *Pf*EF-G_{Mit} was assayed by measuring released inorganic phosphate. One μM EF-G_{Ap} or EF-G_{Mit} was incubated with 5 μM *E.coli* 70S ribosome and 100 μM GDP (Sigma) in the absence or presence of varying concentration of FA (Sigma) at 37°C for 15 min. After incubation, 1 mM GTP lithium salt (Sigma), 1 mM phosphoenol pyruvate (Sigma), 2 μg pyruvate kinase type III (Sigma) and kit contents were added to the reaction mixture and assayed for Pi release. Buffer composition for the GTPase assay was 60 mM Tris-HCl (pH7.6), 30 mM NH_4Cl, 30 mM KCl, 10 mM $MgCl_2$, and 2 mM DTT.

2.5. Nucleotide binding assay

The affinity of EF-G for a non-hydrolyzable analog of GTP (GMPPCP) (Sigma) was determined by fluorescence titration using a LS50B spectrofluorimeter (Perkin Elmer) with a slit band-width of 8 nm for excitation and 6 nm for emission. One μM nucleotide-free EF-G (purified in the presence of 1 mM EDTA to chelate Mg^{2+}) was titrated with increasing concentrations of the nucleotides. Masking of the Trp residue (W72, *E. coli* number) present in the vicinity of the nucleotide binding pocket in EF-G [40] was measured by excitation at 280 nm and recording the emission maxima at 340 nm. All spectra were corrected for buffer containing the corresponding nucleotide concentration. K_d values were determined by plotting $\Delta F/F_{max}$ where F_{max} is Trp fluorescence in the absence of nucleotide and ΔF is the difference between F_{max} and emission maxima at each nucleotide concentration [41]. K_d was calculated by curve-fitting using non-linear regression in GraphPad PRISM software.

2.6. Interaction of EF-G_{Ap} and EF-G_{Mit} with *E. coli* ribosomes

Binding of *Pf*EF-G_{Ap} and *Pf*EF-G_{Mit} to the *E. coli* 70S ribosomes was confirmed by ultra-centrifugation in binding buffer containing 10 mM HEPES-KOH (pH 7.6), 20 mM magnesium acetate, 60 mM NH_4Cl, 6 mM β-ME and 10% glycerol. The reaction mixture (800 µl) contained *Pf*EF-G_{Ap} or EF-G_{Mit} with ribosomes in a ratio of 1:5 and 0.5 mM GTP or 0.5 mM GMPPNP (Sigma). FA (0.5 mM) or thiostrepton (TSP) (50 µM, Sigma) were added and the mixture was incubated at 37°C for 15 min followed by centrifugation at 27,000 rpm for 2 h at 4˚C in a MLA-130 rotor (Beckman). After centrifugation, the supernatant was decanted and the pellet was suspended in SDS-loading buffer. Samples were electrophoresed on SDS-PAG. *Pf*EF-G_{Ap} was detected using anti-EF-G_{Ap} (DI-III) antibody. *Pf*EF-G_{Ap} or *Pf*EF-G_{Mit} ratios with RPS1 were determined after densitometry of Coomassie-stained gels.

2.7. Stopped flow assay for monitoring release of GDP

The kinetics of release of mantGDP (Invitrogen) from *Pf*EF-G_{Ap} mediated by excess unlabelled GDP was investigated by fluorescence stopped-flow measurements on a JASCO J-810 spectro-polarimeter with stopped-flow attachment (SFM-300/S, BioLogic Science Instruments, France) in a buffer containing 60 mM Tris-HCl (pH 7.6), 30 mM NH_4Cl, 30 mM KCl, 10 mM $MgCl_2$, and 2 mM DTT. Nucleotide (GDP) release from ribosome-bound EF-G complex formed with mant-GDP (2 µM), wild type EF-G_{Ap} (2 µM), *E. coli* ribosomes (5 µM) was measured in the presence of varying concentrations of FA (0 µM, 50 µM, 100 µM, 500 µM) with incubation at 37˚C for 30 min. Complexes were transferred to syringe A of the stop-flow device and the chase nucleotide (2.4 mM unlabelled GDP) was loaded into syringe B. Samples from each syringe were rapidly mixed (dead time ~5.7 msec) and injected into the fluorimeter cuvette. Fluorescence (excitation: 360 nm, emission: 444 nm) was monitored over 0-17 sec, with measurement taken over every 5 msec with a band width of 20 nm. 380 nm cut-off filter was used in this experiment. The rate constant (k_i) was determined by fitting the data to an exponential function of the form $y(t)= at + b + \Sigma A_i e^{-k_i.t}$ where y is the fluorescence at time t and the slope (a) and offset (b) correspond to the linear drift after the reaction; the best-fitting amplitude (A_i) and apparent dissociation rate constant (K_d) were determined with the Bio-Kine software (BioLogic).

Table 1. IC_{50} of fusidic acid for the first and second infection cycle

Time (h)	IC50 ± S.D.a
48	45.7 ± 3.5 M
96	23.8 ± 2.8 M

*average of three determinations

3. Results

3.1. Molecular modeling of *P. falciparum* organellar EF-Gs and their FA interaction sites

Inhibition of *P. falciparum* growth in erythrocytes by FA does not exhibit the classic ‘delayed-death’ phenotype observed for apicoplast-targeted proteins. Delayed-death is a phenomenon wherein parasite development is inhibited in the second cycle of erythrocytic infection [8, 9]. FA inhibited parasite growth both in the first as well as the second cycle of infection of *P. falciparum* (3D7) parasites in blood culture. IC_{50} of the drug in the first and second cycles was

determined to be 45.7±3.5 μM and 23.8±2.8 μM, respectively (Table 1). These values are comparable to those reported by Johnson et al. [18] who determined the IC_{50} of FA to be 52.8±2.5 μM for the first cycle and 36.6±2.4 μM for the second cycle of infection. The inhibitory effect of FA on parasite growth was primarily manifested in progression of rings to trophozoites evident across 8 to 16 h post treatment, with FA-treated (28 μM and 93 μM) parasites stalled at the ring stage (Supplementary Figure S1). A lag in parasite stage progression was subsequently seen at all times in the presence of 28 μM drug and no live parasites were observed in 93 μM drug by 32 h post treatment. The early inhibitory effect observed with FA suggested that the drug may target other sites in addition to apicoplast EF-G, of which mitochondrial EF-G is an obvious candidate. Thus, the action of FA on apicoplast EF-G was determined and compared with its effect on the mitochondrial factor.

P. falciparum nuclear genes PF3D7_0602400 and PF3D7_1233000 (PlasmoDB: www.plasmodb.org) encode EF-G targeted to the apicoplast and mitochondrion, respectively [18]. ClustalW alignment with bacterial and organellar EF-Gs shows extensive conservation in the GTPase domain of both the *Plasmodium* proteins (Supplementary Figure S2). On the basis of identified N-terminal organelle targeting elements, the predicted processed form (with the organelle targeting sequence removed) of *Pf*EF-G_{Ap} is of ~97 kDa and processed *Pf*EF-G_{Mit} is predicted to be ~88 kDa. The larger apicoplast version contains insertions positioned in the region between domains I and II and within domain IVa. The crystal structure of *T. thermophilus* EF-G bound to FA has been reported [33]. *Tt*EF-G shares 33.43% and 30.28% sequence identity with *Pf*EF-G_{Ap} and *Pf*EF-G_{Mit}, respectively. In order to understand structural properties of the proteins, molecular modeling of *P. falciparum* EF-G_{Ap} and EF-G_{Mit} was carried out on the crystal structure *Tt*EF-G [33]. Structural folds in all domains were largely conserved although *Pf*EFG_{Ap} and *Pf*EF-G_{Mit} insertion sequences appeared as loops and could not be modelled on any other known structure (Fig. 1A). *Pf*EF-G_{Ap} has three insertions of 62 aa (between DI and DII), 41 aa (in DII) and 39 aa (in DIVa) and *Pf*EF-G_{Mit} has two insertions of 42 aa (between DI and DII) and 13 aa (ni DII) (Fig. 1A).

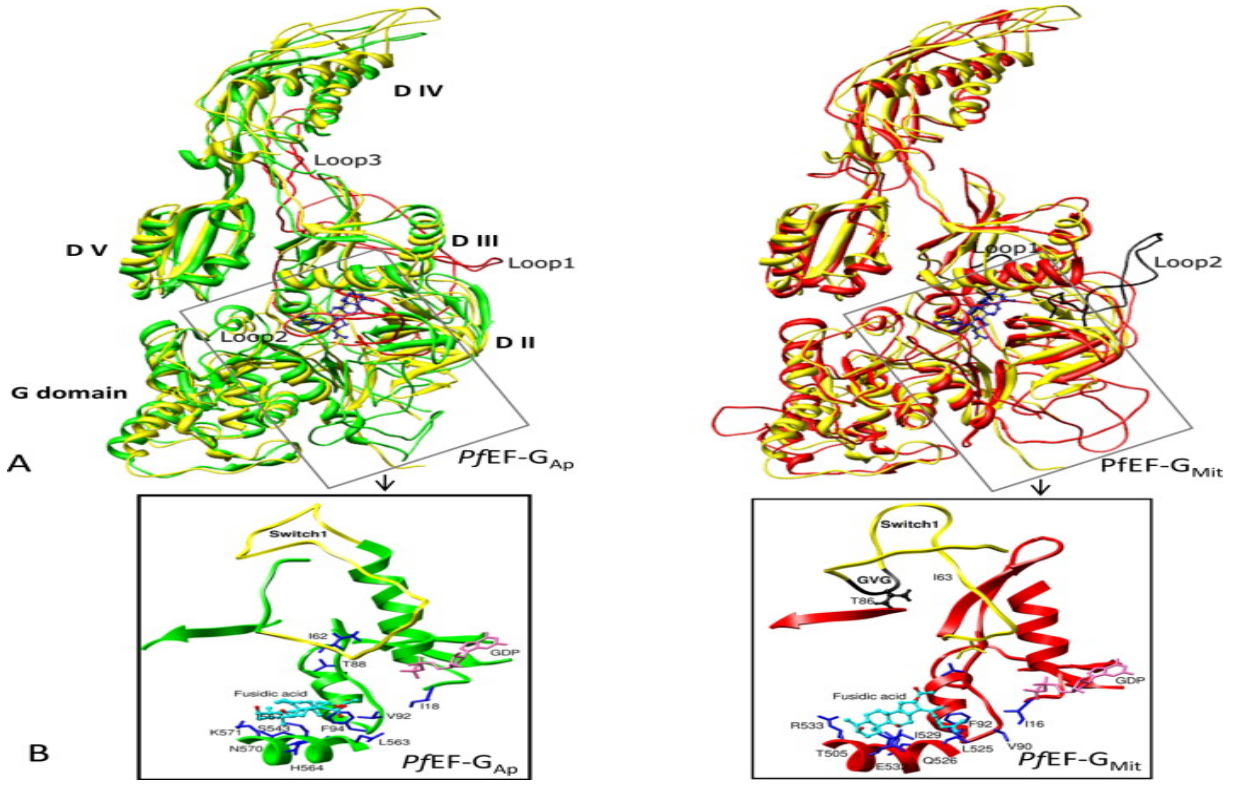

Fig. 1. Structure prediction and docking of FA. (A) ***Pf***EF-G_{Ap} (green) and ***Pf***EF-G_{Mit} (red) modeled on the crystal structure of ***Thermus thermophilus*** EF-G (yellow). Large sequence insertions in the ***Plasmodium*** proteins are shown as loops (red and black in the ***Pf***EF-G_{Ap} and ***Pf***EF-G_{Mit} models, respectively). (B) FA docked onto ***Pf***EF-G_{Ap} and ***Pf***EF-G_{Mit}. A region of ***Pf***EF-G_{Ap} and ***Pf***EF-G_{Mit} from (A) is enlarged in (B) with change in orientation for better clarity. Amino acids involved in major interactions with FA are shown. The switch I loop is in yellow with the GVG insertion indicated in ***Pf***EF-G_{Mit}. (For interpretation of the references to color in this figure legend, the reader is referred to the web version of the article.)

The affinity of FA with organellar EF-Gs was assessed by prediction of the energy of FA binding to the receptor (EF-G) site carried out using AUTODOCK3 [39]. Data on the FA binding site across the *Pf*EF-G_{Ap} and *Pf*EF-G_{Mit} surface were obtained from the *Tt*EF-G template. Coordinates of the bound GDP in the template structure were extracted and assigned at similar positions in the *Pf*EF-G_{Ap} and *Pf*EF-G_{Mit} models (Fig. 1B). FA was re-docked onto the *Tt*EF-G structure; the RMSD between the crystal-bound and docked FA conformations in the receptor active site was as low as 0.7 Å and the docking energy was -7.99 kcal/mol. Further, FA was docked in both *Pf*EF-G_{Ap} and *Pf*EF-G_{Mit} models and the binding energy of FA was estimated to be -6.55 kcal/mol and -5.35 kcal/mol for *Pf*EF-G_{Ap} and *Pf*EF-G_{Mit}, respectively. FA acquired similar conformation in both *Pf*EF-G_{Ap} and *Pf*EF-G_{Mit} models as in *Tt*EF-G. Important interactions made by FA with the *Pf*EF-G_{Ap} binding site were through I62, T88, I18, V92, F94, H564, S543, L563, N570, K571 and major interactions between FA and *Pf*EF-G_{Mit} were through I63, T86, F92, I16, V90, L525, I529, E532, Q526, R533, T505 (Fig. 1B).

3.2. EF-G_{Ap} and EF-G_{Mit} exhibit intrinsic GTPase activity

*Pf*EF-G_{Ap} was expressed as a recombinant protein in *E. coli*. The region covering domains I-III (aa 89 to 680) was first cloned in fusion with an N-terminal 6XHis tag, expressed and purified,

and antibodies were generated against this protein (*Pf*EF-G_{Ap}DI-III) (Supplementary Figure S3). The anti-EFG_{Ap} antibody recognised a band corresponding to the expected size of processed EF-G_{Ap} (~97 kDa) in the parasite lysate (Supplementary Figure S3). The recombinant apicoplast and mitochondrial EF-Gs containing all domains but lacking organelle targeting elements (processed forms) were cleaved to remove the N-terminal GST-tag and purified as ~97 kDa (*Pf*EF-G_{Ap}) and ~88 kDa (*Pf*EF-G_{Mit}) proteins (supplementary data in [26]).

The GTPase activity of the EF-Gs was measured spectrophotometrically. Both *Pf*EF-G_{Ap} and *Pf*EF-G_{Mit} hydrolysed GTP in a protein concentration dependent manner (Fig. 2A). The affinity of the organellar factors for GTP was estimated by fluorescence quenching using a non-hydrolyzable analog of GTP (GMPPNP) (Fig. 2B). *Pf*EF-G_{Ap} and *Pf*EF-G_{Mit} have similar binding affinity for GTP (K_d values of the two proteins for GMPPNP were ~80 µM and 68 µM, respectively). This is in the same range as the reported K_d value (94 µM) of *E. coli* EF-G for GMPPNP [42].

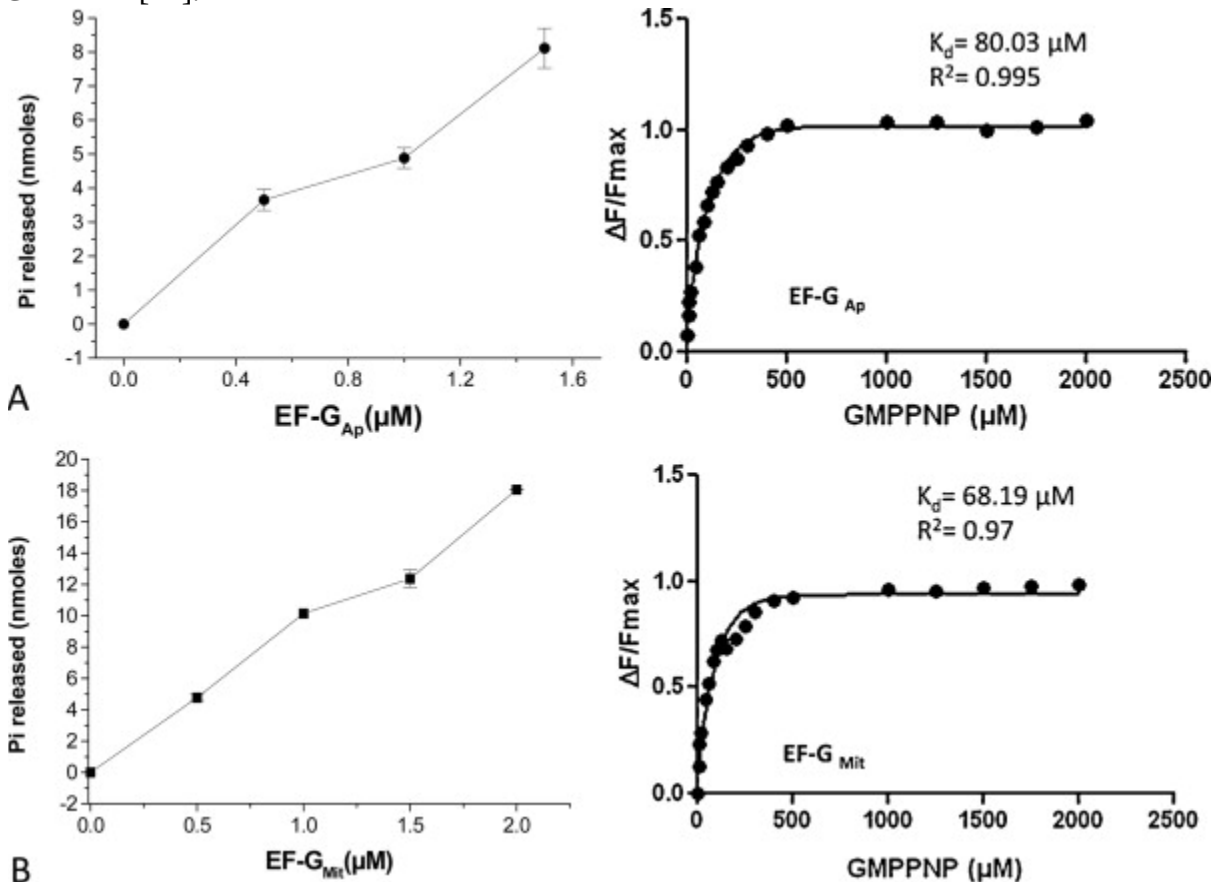

Fig. 2. GTP binding and hydrolysis by *P. falciparum* EF-Gs. GTPase activity of purified *Pf*EF-G_{Ap} and *Pf*EF-G_{Mit} as a function of enzyme concentration (left panel in A and B). Determination of the affinity of *Pf*EF-G_{Ap} and *Pf*EF-G_{Mit} with GMPPNP. K_d values derived from the experiment are shown in the plot (right panel in A and B).

3.3. Fusidic acid (FA) targets apicoplast translation and EF-G_{Ap}

The effect of FA on apicoplast versus cytoplasmic translation in *P. falciparum* was investigated by determining the impact of FA treatment on levels of apicoplast-encoded SufB (PlasmoDB ID: PFC10_API0012) and nuclear-encoded tubulin (α-tubulin 1 &2, PlasmoDB ID:

PF3D7_0903700 and PF3D7_0422300). Levels of the two proteins were determined by immunoblots of parasite lysates from equal numbers of parasites prepared 28 h post-treatment and developed using antibodies against the two proteins [28]. SufB levels decreased at 28 µM and 93 µM of FA (Fig. 3A). The decrease in SufB/tubulin ratio indicated a drastic fall in apicoplast translation upon FA treatment.

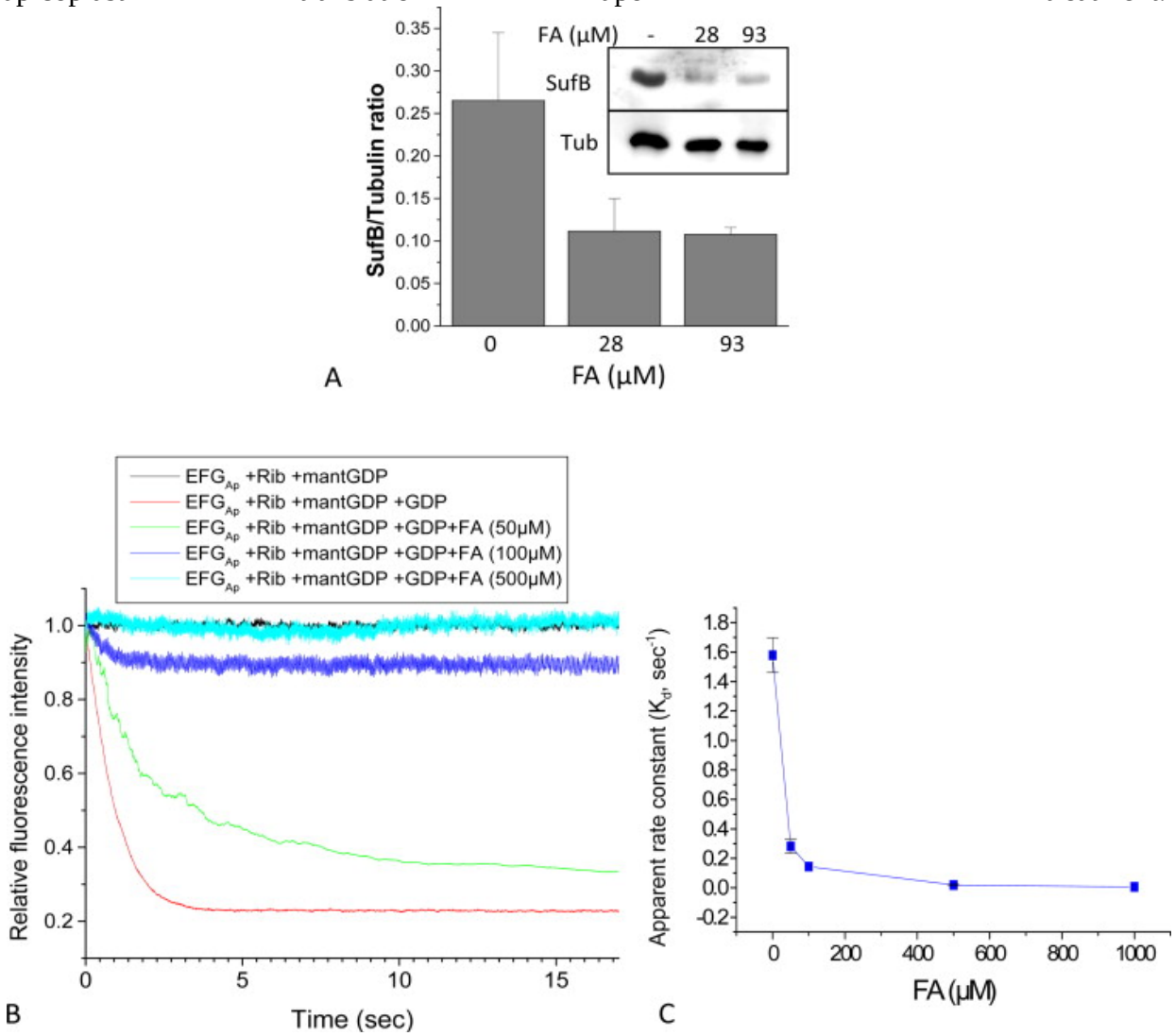

Fig. 3. Effect of FA on apicoplast translation and release of *Pf*EF-G_{Ap} from the ribosome. (A) Inhibition of apicoplast translation by FA (28 and 93 µM) as measured from levels of apicoplast-encoded SufB detected in Western blots using anti-EF-Tu Ab. SufB/tubulin ratio inferred from the western blot is shown in the plot. (B) FA prevents release of *Pf*EF-G_{Ap}·GDP from the ribosome. Fluorescence stopped flow rapid kinetic measurements of mant-GDP release from the *Pf*EF-G_{Ap}·mant-GDP complex upon addition of excess unlabeled GDP (2.4 mM) in the presence or absence of FA. Ribosome (5 µM), 2 µM mant-GDP and 2 µM *Pf*EF-G_{Ap} were present in all reactions. The effect of increasing concentrations of FA on locking of the *Pf*EF-G_{Ap}·mant-GDP complex on the ribosome is seen. Time course profile obtained by averaging three individual transients is shown. (C) Apparent dissociation rate constants of the data shown in (B).

It is known that FA inhibits translation by trapping EF-G in its GDP-bound form with the ribosome after GTP hydrolysis [33, 43]. To examine the inhibitory effect of FA on the release of *Pf*EF-G_{Ap}.GDP from the ribosome, fluorescent complexes of *Pf*EF-G_{Ap}, mant-GDP (fluorophore tagged GDP) and surrogate *E. coli* ribosomes were formed in the absence or presence of varying concentration of FA. The rate of release of mant-GDP was observed by chasing these complexes with excess of unlabelled GDP (Fig. 3B). In the absence of FA, rapid release of mant-GDP with dissociation rate constant (K_d) = 1.58 ± 0.118 sec^{-1} was observed by monitoring fluoresence decrease over time. On the addition of FA, the release of mant-GDP was inhibited in a drug concentration dependent manner from 50 µM FA (K_d = 0.28 ± 0.046 sec^{-1}) to 500 µM FA (K_d = 0.0189 ± 0.0035 sec^{-1}) (Fig. 3B and C). Thus FA inhibited the release of mant-GDP from the *Pf*EF-G_{Ap}.mant-GDP.ribosome complex indicating that it could lock the *Pf*EF-G_{Ap}.GDP form onto the pre-translocation ribosome after GTP hydrolysis.

3.4. FA has a greater inhibitory effect on EF-G_{Ap} compared to EF-G_{Mit}

Since FA clearly mediated locking of the apicoplast EF-G.GDP form onto the ribosome, we also evaluated its effect on the mitochondrial factor. Locking of EF-G onto the ribosome was monitored by co-sedimentation of the factor with ribosomes after high-speed centrifugation. Ribosomes, EF-G and GTP/GMPPNP were incubated with FA or thiostrepton. The retention of EF-G on the ribosome was quantified by calculating the relative ratios of *Pf*EF-G_{Ap} or *Pf*EF-G_{Mit} and ribosomal subunit (Rps1) band intensities (Fig. 4). *Pf*EF-G_{Ap} was clearly trapped in a ribosome-bound form in the presence of both FA (six times more *Pf*EF-G_{Ap} was ribosome-bound compared to the without drug control) and GMPPNP. Thiostrepton did not have any effect on retention of *Pf*EF-G_{Ap} on the ribosome. This is similar to observations made with *E. coli* EF-G [44]. On the other hand, FA influenced *Pf*EF-G_{Mit} to a lower extent; On an average from three repeat experiments, ~3.5 times more EF-G_{Mit} was ribosome-bound compared to the without drug control. Surprisingly, significant locking of *Pf*EF-G_{Mit} to the ribosome was also seen in the presence of thiostrepton, which is known to inhibit bacterial protein biosynthesis by binding to the GTPase-associated center on the 50S subunit. Thiostrepton has been reported to dually target apicoplast translation and the proteasome in *Plasmodium* [45]. Our observation suggests additional action of this drug on mitochondrial EF-G.

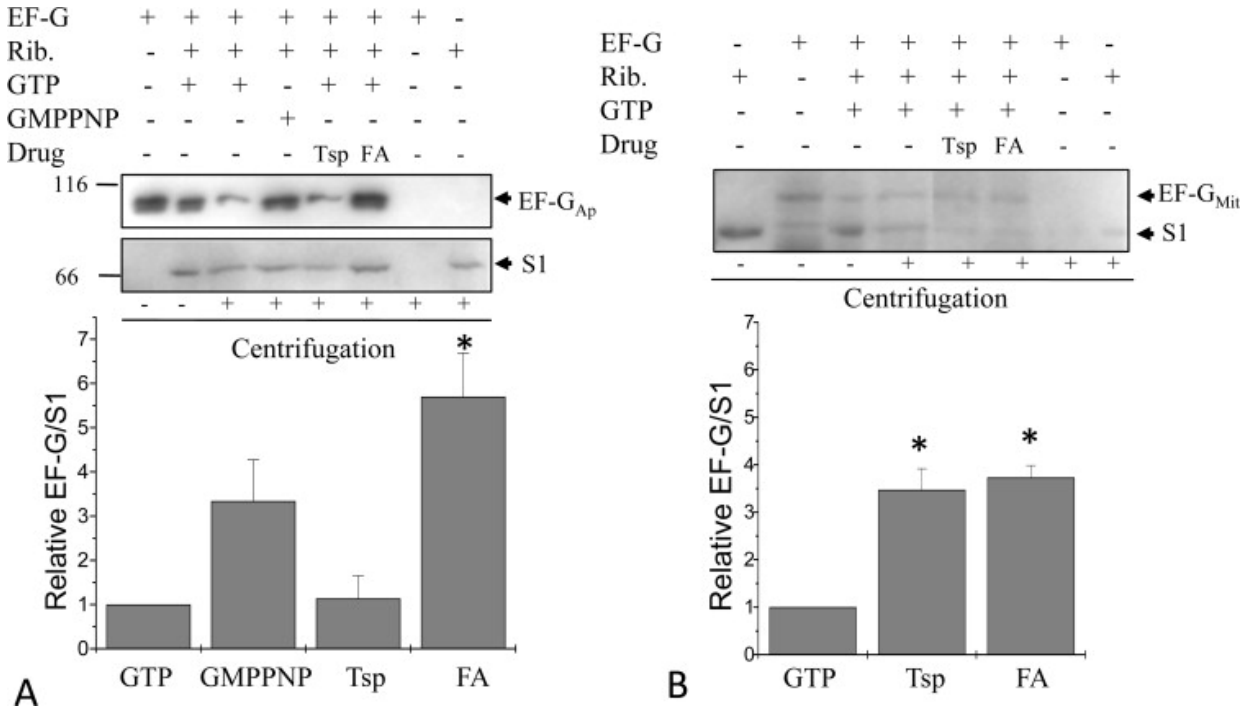

Fig. 4. The effect of FA and thiostrepton on retention of P. falciparum EF-G·GDP on the ribosome. (A) Ribosome-bound PfEF-GAprecovered after ultracentrifugation wasdetected by western blot using anti-PfEF-GAp(DI–III) Ab. Levels of the ribsomal subunit S1 as seen upon Coomassie staining are shown in the lower panel. Relative PfEF-GAp/S1 ratios are plotted. (B) Ribosome-bound PfEF-GMitand ribosomal subunit S1 detected by Coomassie staining and the plot of PfEF-GMit/S1 ratio.* denotes significantdifferences between ribosome-bound EF-G in the absence or presence of drug at $P < 0.05.0$

We next evaluated inhibition of ribosome dependent multi-turnover GTPase activity of *P. falciparum* organellar EF-Gs in the presence of varying concentrations of FA. GTP hydrolysis by *Pf*EF-G_{Ap} decreased under increasing concentrations of FA and was completely abolished at 200 µM of the drug (Fig. 5). In contrast, GTP hydrolysis by *Pf*EF-G_{Mit} was inhibited by only ~50% in the presence on 200 µM FA. Thus FA inhibits apicoplast EF-G but only has a minimal effect on ribosomal locking of mitochondrial EF-G.GDP as well as ribosome-dependent multi-turnover GTP hydrolysis by the mitochondrial factor.

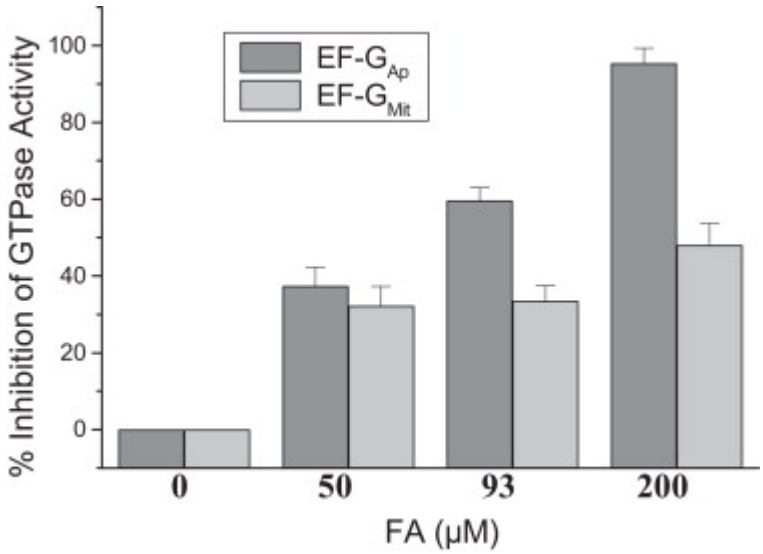

Fig. 5. FA-mediated inhibition of multi-turnover GTP hydrolysis in the presence of ribosome by *Pf*EF-G_{Ap} and *Pf*EF-G_{Mit}. The reactions contained 1 μM each of *Pf*EF-G_{Ap} and *Pf*EF-G_{Mit} with increasing concentrations of FA

A three amino acid insertion in the switch I region of mitochondrial EF-G alters inhibition by FA

The crystal structure of *T. thermophilus* post-translocation ribosome complexed with EF-G and FA [33] identifies an FA binding pocket in EF-G surrounded by the switch II region of the G domain, as well as domains II and III. This location of FA is consistent with mutational data that map FA resistance and hypersensitivity mutations in this region [46, 47]. The FA-EG-G crystal structure [33] also indicates that FA would clash with the switch I loop in its closed conformation as in the GTP-bound form of EF-G and that FA binding must require a disordered, open form of switch I [33]. Primary sequence comparison of the two *P. falciparum* organellar EF-Gs and sensitive bacterial EF-G proteins is unable to identify clear differences with known effects on FA action between the mitochondrial and apicoplast factors [18]. We thus looked for other elements in mitochondrial EF-G that may contribute to the relative refractivity of *Pf*EF-G_{mit} to inhibition by FA. Sequence comparison and phylogeny of mitochondrial EF-Gs has shown that the mtEFG-1 clade is characterised by the presence of a small well conserved insertion, with the consensus sequence GVG, in the switch I region [25]. The GVG sequence is exclusive to mtEF-G1 sequences and is not found on any plastid/apicoplast EF-G (Fig. 6A). Considering the importance of an open switch I loop in FA binding, the ability of the GVG motif found in mtEFG-1 proteins including *Pf*EF-G_{Mit} to alter the sensitivity of the mitochondrial factor to FA was investigated.

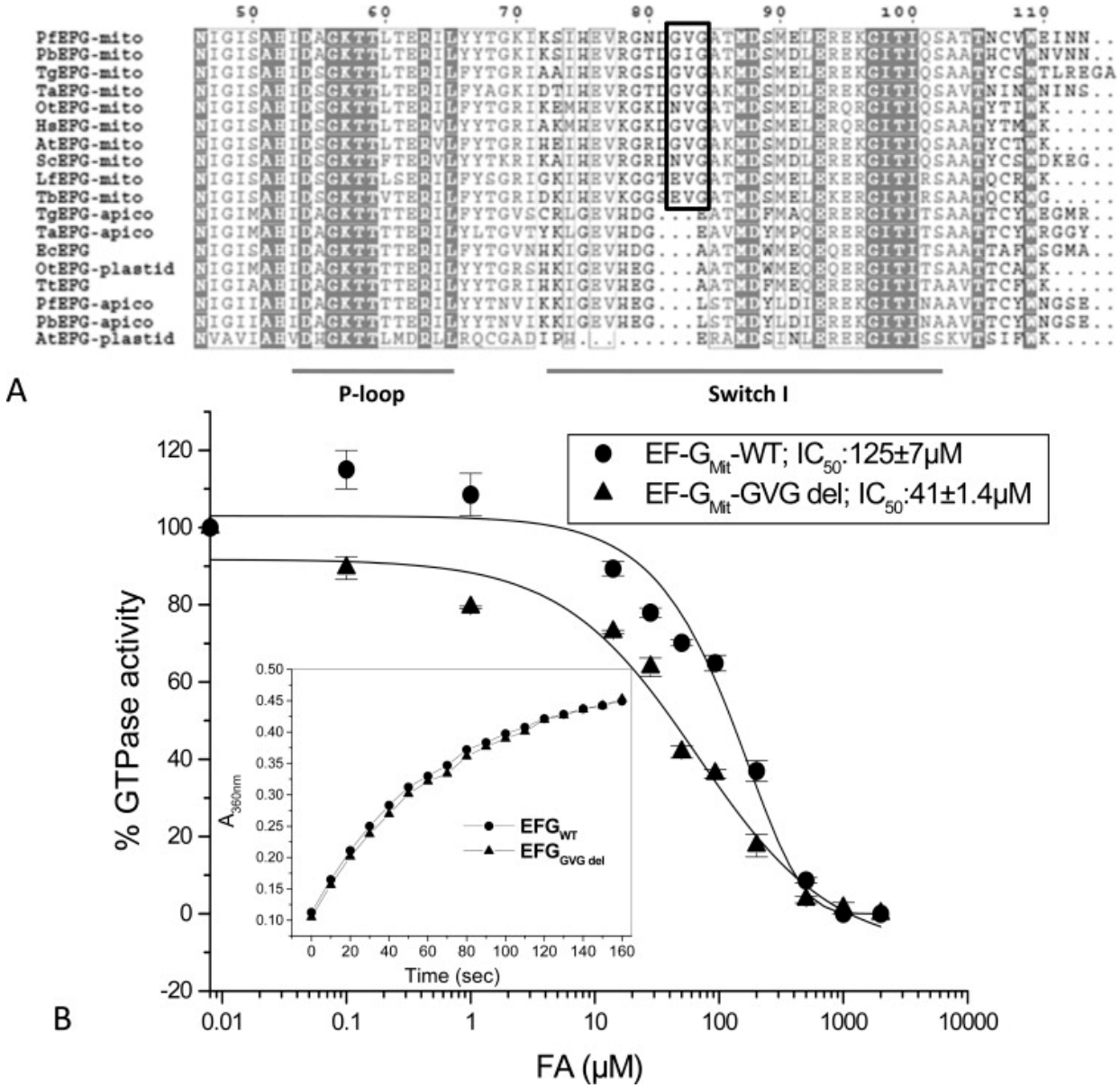

Fig. 6. Effect of the switch I GVG motif of *Pf*EF-G$_{Mit}$ on inhibition by FA. (A) A section of the ClustalW alignment of bacterial, plastid and mitochondrial EF-G1 proteins. The GVG insertion is outlined in black. Pf, *P. falciparum*; Pb, *P. berghei*; Tg, *Toxoplama gondii*; Ta, *Theileria annulata*; Ot, *Ostreococcus tauri*; Hs, *Homo sapiens*; At, *Arabidopsis thaliana*; Sc, *Saccharomyces cerevisiae*; Lf, *Leishmania major* (strain Friedlin); Tb, *Trypanosoma brucei*; Ec, *Escherichia coli*; Tt, *Thermus thermophilus*. (B) The effect of increasing concentrations of FA on multi-turnover GTP hydrolysis by *Pf*EF-G$_{Mit}$ and *Pf*EF-G$_{Mit}$GVGdel. Inset shows multiple substrate turnover GTPase activity of the two proteins in the absence of drug.

Recombinant *Pf*EF-G$_{Mit}$ lacking the GVG motif (*Pf*EF-G$_{mit}$GVGdel) was expressed in *E. coli* and the purified (Supplementary Figure S2), GST-tag cleaved protein was compared with the wild type factor in a multi-turnover GTP hydrolysis assay in the presence of ribosome and increasing concentrations of FA (Fig. 6B). The two proteins had comparable GTPase activity in the absence of the drug (Fig. 6B, inset). However, FA had a greater inhibitory effect on *Pf*EF-

G_{Mit}GVGdel compared to wild type *Pf*EF-G_{Mit}; the IC_{50} values for FA inhibition of *Pf*EF-G_{Mit}GVGdel and *Pf*EF-G_{Mit} were significantly different ($P=3.42\ e^{-5}$) and were determined to be 41 ± 1.4μM and 125 ± 7μM, respectively thus indicating that deletion of the GVG motif promoted access and binding of FA to the mitochondrial factor. The IC_{50} of FA for *Pf*EF-G_{Ap} was determined to be 75.5 ± 7.6 μM (data not shown), also indicating that *Pf*EF-G_{Mit} was less sensitive to FA than the apicoplast factor.

4. Discussion

P. falciparum apicoplast and mitochondrial EF-G homologs have structural domains DI to DV conserved across species. *Pf*EF-G_{Ap} and *Pf*EF-G_{Mit} exhibit GTPase activity required for translocation and also function with the relevant organellar RRF to mediate ribosome recycling in the mitochondrion and apicoplast of the parasite [26]. Docking of FA on the structural model of *P. falciparum* organellar EF-Gs predicted comparable interaction energy of the drug with both factors with a slightly lower dock score for *Pf*EF-G_{Mit} (-6.55 kcal/mol and -5.35 kcal/mol for *Pf*EF-G_{Ap} and *Pf*EF-$G_{Mit,}$ respectively). However, locking of EF-G.GDP onto the ribosome by FA as well as inhibition of multi-substrate turnover GTP hydrolysis was higher for *Pf*EF-G_{Ap} indicating that FA has a more pronounced effect on the apicoplast factor. The action of FA on both organellar EF-Gs in *P. falciparum* explains the observed inhibition of intraerythrocytic parasite growth in the first cycle (IC_{50}: 46 μM) that would be a manifestation of inhibition of mitochondrial translation. This would be combined with effects of the more potent inhibition of apicoplast translation in the second infection cycle that is seen as a reduction in IC_{50} (~24 μM) of the drug. The IC_{50} of FA for inhibition of EF-G of *S. aureus* assayed by tripeptide synthesis is 100 μM [48], a value close to the IC_{50} range (10 to 100 μM) reported for *E. coli* EF-G using poly(Phe) synthesis and GTPase turnover assays [43, 49-51]. FA IC_{50} determined for the two *Plasmodium* EF-Gs by GTPase turnover is similar to these values, thus strengthening the view that organelle EF-Gs are targets of the drug in *P. falciparum* and are primarily responsible for growth inhibition of the parasite by FA.

The antibiotics FA and thiostrepton inhibit EF-G but in different ways. FA stalls the EFG.GDP complex on the ribosome by binding to EF-G.GDP immediately after GTP hydrolysis and inhibiting a conformational change required for release of the factor from the ribosome [43, 52]. It has been shown that the antibacterial activity of FA is primarily due to its inhibition of ribosome recycling, possibly by inhibition of a conformational transition of EF-G, which is enhanced by RRF, and drives ribosome subunit dissociation [51]. Thiostrepton affects EF-G by binding in the GTPase-associated regions of the 50S subunit [53] and prevents the stable binding of EF-G to the ribosome [54]. It thus greatly reduces ribosome dependent GTPase activity of the factor. As reported for *E. coli* EF-G [44], thiostrepton did not stall *Pf*EF-G_{Ap} on the *E. coli* ribosome in the presence of excess GTP. However, it enhanced retention of *Pf*EF-G_{Mit} on the ribosome under identical conditions. As seen with FA, thiostrepton induces early parasite killing and does not exhibit a ‘delayed-death’ phenotype typical of apicoplast-specific inhibitors [8]. Anti-parasitic action of thiostrepton on *P. falciparum* has been largely attributed to dual targeting of apicoplast translation and the proteasome [45]. Recent global gene expression data has suggested that the drug acts on parasite mitochondrial translation possibly by inhibition of mitochondrial ribosome function [55]. Although the *P. falciparum* apicoplast 23S rRNA is reported to be the preferred interaction site for thiostrepton [56], our results indicate that thiostrepton can act on the EF-G_{Mit}-ribosome interface in the parasite mitochondrion, thus also inhibiting mitochondrial translation.

Resistance to FA has been mapped to more than 40 residues in bacterial EF-Gs [57-60]. These mutations involve residues in direct contact with FA, or those that shape the drug binding pocket; others influence EF-G–ribosome interactions, alter interdomain orientation of EF-G, or decrease structural stability of domains II and III of the factor [47, 48, 60]. Primary sequence comparison of *Pf*EF-G_{Ap} and *Pf*EF-G_{Mit} to look for differences in known residues associated with FA sensitivity is unable to yield specific conclusions regarding differences in FA susceptibility of the two factors [18]. An obvious difference in the sequence of the two organellar EF-Gs is the presence of the GVG motif in the switch I region of *Pf*EF-G_{Mit} that is a conserved and exclusive feature of mtEF-G1 proteins, and our results establish that this decreases the sensitivity of the mitochondrial factor to FA. Removal of the GVG motif in *Pf*EF-G_{Mit}, enhanced inhibition by FA (about 3-fold reduction in IC_{50}). The lower sensitivity of *Pf*EF-G_{Mit} compared to apicoplast EF-G (IC_{50} of ~125 µM for *Pf*EF-G_{Mit} and ~75 µM for *Pf*EF-G_{Ap}) could be due to a GVG-induced change in the structure of the switch I loop proximal to the FA binding site. The switchI loop is required to be in an open, disordered configuration for FA to be able to access the factor, as in the GDP-bound form of EF-G. As reported by Gao et al. [33], its closed conformation in the GTP-bound form of EF-G would clash with FA, thus also suggesting that the binding of FA must occur after GTP hydrolysis. The presence of the GVG insertion in switchI of *Pf*EF-G_{Mit} (Fig. 1) lowers the disorder in the region as predicted by PrDOS (http://prdos.hgc.jp; [61]) [Supplementary Figure S4] and could alter or stiffen the conformation of the open loop, thus interfering with FA binding. This observation also has implications in understanding the effect of FA treatment on other mtEF-G1 proteins that carry the GVG insertion and would possibly show reduced sensitivity to FA. In fact, the GTPase and translocation activities of human mtEF-G1 are not inhibited by FA [24, 62]; the GVG insertion in human mtEF-G1 might contribute to this resistance.

The search for organellar translation inhibitors as possible anti-malarials is confounded by the possibility of off-targets at other locations in the parasite. The evaluation of the precise target-specific activities of selected inhibitors/antibiotics helps identify primary sites of action that would aid in design of additional lead molecules and derivatives. Our results identify apicoplast EF-G as the primary site of action of FA, provide an explanation for reduced sensitivity of mitochondrial EF-G to the drug, and indicate that thiostrepton also targets the mitochondrial EF-G-ribosome interface in *P. falciparum*.

Acknowledgements

We thank Dr. P Guptasarma for help with stop-flow fluorimetry and Prof. Umesh Varshney for *E. coli* MRE600 strain. SB, AG, SV and US received scholarships from the University Grants Commission and the Council for Scientific and Industrial Research, Government of India. This work was funded by CSIR network project Splendid (BSC0104i) and project Mephitis of the European Community's Seventh Framework Programme (FP7/ 2007-2013) under the grant agreement number HEALTH-F3-2009-223024. **This is CSIR-CDRI communication no. 8561.**

Appendix A: Supplementary Data

Supplementary data associated with this article can be found,in the online version, at http://dx.doi.org/10.1016/j.molbiopara.2013.10.003.

References

[1] Lim L, McFadden GI. The evolution, metabolism and functions of the apicoplast. Philosophical Transactions of the Royal Society of London B: Biological Sciences 2010;365:749-63.
[2] Botte CY, Dubar F, McFadden GI, Marechal E, Biot C. *Plasmodium falciparum* apicoplast drugs: targets or off-targets? Chemical Reviews 2012;112:1269-83.
[3] Yeh E, DeRisi JL. Chemical rescue of malaria parasites lacking an apicoplast defines organelle function in blood-stage *Plasmodium falciparum*. PLoS Biology 2011;9:e1001138.
[4] van Dooren GG, Marti M, Tonkin CJ, Stimmler LM, Cowman AF, McFadden GI. Development of the endoplasmic reticulum, mitochondrion and apicoplast during the asexual life cycle of *Plasmodium falciparum*. Molecular Microbiology 2005;57:405-19.
[5] Stanway RR, Mueller N, Zobiak B, Graewe S, Froehlke U, Zessin PJ, et al. Organelle segregation into *Plasmodium* liver stage merozoites. Cellular Microbiology 2011;13:1768-82.
[6] Raghu Ram EV, Kumar A, Biswas S, Chaubey S, Siddiqi MI, Habib S. Nuclear gyrB encodes a functional subunit of the *Plasmodium falciparum* gyrase that is involved in apicoplast DNA replication. Molecular and Biochemical Parasitology 2007;154:30-9.
[7] Dar MA, Sharma A, Mondal N, Dhar SK. Molecular cloning of apicoplast-targeted *Plasmodium falciparum* DNA gyrase genes: unique intrinsic ATPase activity and ATP-independent dimerization of PfGyrB subunit. Eukaryotic Cell 2007;6:398-412.
[8] Goodman CD, Su V, McFadden GI. The effects of anti-bacterials on the malaria parasite *Plasmodium falciparum*. Molecular and Biochemical Parasitology 2007;152:181-91.
[9] Dahl EL, Rosenthal PJ. Apicoplast translation, transcription and genome replication: targets for antimalarial antibiotics. Trends in Parasitology 2008;24:279-84.
[10] Ruangweerayut R LS, Hutchinson D, Chauemung A, Banmairuroi V, Na-Bangchang K. Assessment of the pharmacokinetics and dynamics of two combination regimens of fosmidomycin-clindamycin in patients with acute uncomplicated *falciparum* malaria. Malaria Journal 2008;7:225.
[11] Borrmann S, Lundgren I, Oyakhirome S, Impouma B, Matsiegui PB, Adegnika AA, et al. Fosmidomycin plus clindamycin for treatment of pediatric patients aged 1 to 14 years with *Plasmodium falciparum* malaria. Antimicrobial Agents and Chemotherapy 2006;50:2713-8.
[12] Camps M, Arrizabalaga G, Boothroyd J. An rRNA mutation identifies the apicoplast as the target for clindamycin in *Toxoplasma gondii*. Molecular Microbiology 2002;43:1309-18.
[13] Stanway RR, Witt T, Zobiak B, Aepfelbacher M, Heussler VT. GFP-targeting allows visualization of the apicoplast throughout the life cycle of live malaria parasites. Biology of the Cell 2009;101:415-30, 5 p following 30.
[14] Vaidya AB, Mather MW. Mitochondrial evolution and functions in malaria parasites. Annual Review of Microbiology 2009;63:249-67.
[15] Jackson KE, Habib S, Frugier M, Hoen R, Khan S, Pham JS, et al. Protein translation in *Plasmodium* parasites. Trends in Parasitology 2011;27:467-76.
[16] Clough B, Rangachari K, Strath M, Preiser PR, Wilson RJ. Antibiotic inhibitors of organellar protein synthesis in *Plasmodium falciparum*. Protist 1999;150:189-95.
[17] Biswas S, Lim EE, Gupta A, Saqib U, Mir SS, Siddiqi MI, et al. Interaction of apicoplast-encoded elongation factor (EF) EF-Tu with nuclear-encoded EF-Ts mediates translation in the *Plasmodium falciparum* plastid. International Journal for Parasitology 2011;41:417-27.
[18] Johnson RA, McFadden GI, Goodman CD. Characterization of two malaria parasite organelle translation elongation factor G proteins: the likely targets of the anti-malarial fusidic acid. PLoS One 2011;6:e20633.

[19] Jones RN, Mendes RE, Sader HS, Castanheira M. In vitro antimicrobial findings for fusidic acid tested against contemporary (2008-2009) gram-positive organisms collected in the United States. Clinical Infectious Disease 2011;52 Suppl 7:S477-86.
[20] Agrawal RK, Heagle AB, Penczek P, Grassucci RA, Frank J. EF-G-dependent GTP hydrolysis induces translocation accompanied by large conformational changes in the 70S ribosome. Nature Structural Biology 1999;6:643-7.
[21] Nyborg J, Nissen P, Kjeldgaard M, Thirup S, Polekhina G, Clark BF. Structure of the ternary complex of EF-Tu: macromolecular mimicry in translation. Trends in Biochemical Sciences 1996;21:81-2.
[22] Gao N, Zavialov AV, Ehrenberg M, Frank J. Specific interaction between EF-G and RRF and its implication for GTP-dependent ribosome splitting into subunits. Journal of Molecular Biology 2007;374:1345-58.
[23] Tsuboi M, Morita H, Nozaki Y, Akama K, Ueda T, Ito K, et al. EF-G2mt is an exclusive recycling factor in mammalian mitochondrial protein synthesis. Molecular Cell 2009;35:502-10.
[24] Suematsu T, Yokobori S, Morita H, Yoshinari S, Ueda T, Kita K, et al. A bacterial elongation factor G homologue exclusively functions in ribosome recycling in the spirochaete *Borrelia burgdorferi*. Molecular Microbiology 2010;75:1445-54.
[25] Atkinson GC, Baldauf SL. Evolution of elongation factor G and the origins of mitochondrial and chloroplast forms. Molecular Biology and Evolution 2010;28:1281-92.
[26] Gupta A, Mir SS, Jackson KE, Lim EE, Shah P, Sinha A, et al. Recycling factors for ribosome disassembly in the apicoplast and mitochondrion of *Plasmodium falciparum*. Molecular Microbiology 2013;88:891-905.
[27] Singh S, Srivastava RK, Srivastava M, Puri SK, Srivastava K. In-vitro culture of *Plasmodium falciparum*: utility of modified (RPNI) medium for drug-sensitivity studies using SYBR Green I assay. Experimental Parasitology 2011;127:318-21.
[28] Kumar B, Chaubey S, Shah P, Tanveer A, Charan M, Siddiqi MI, et al. Interaction between sulphur mobilisation proteins SufB and SufC: evidence for an iron-sulphur cluster biogenesis pathway in the apicoplast of *Plasmodium falciparum*. International Journal for Parasitology 2011;41:991-9.
[29] Sali A, Blundell TL. Comparative protein modelling by satisfaction of spatial restraints. Journal of Molecular Biology 1993;234:779-815.
[30] Sali A, Overington JP. Derivation of rules for comparative protein modeling from a database of protein structure alignments. Protein Science 1994;3:1582-96.
[31] Sali A, Potterton L, Yuan F, van Vlijmen H, Karplus M. Evaluation of comparative protein modeling by MODELLER. Proteins 1995;23:318-26.
[32] Sali A. Modeling mutations and homologous proteins. Current Opinions in Biotechnology 1995;6:437-51.
[33] Gao YG, Selmer M, Dunham CM, Weixlbaumer A, Kelley AC, Ramakrishnan V. The structure of the ribosome with elongation factor G trapped in the posttranslocational state. Science 2009;326:694-9.
[34] Li SC. The difficulty of protein structure alignment under the RMSD. Algorithms for Molecular Biology 2013;8:1.
[35] Carugo O, Pongor S. A normalized root-mean-square distance for comparing protein three-dimensional structures. Protein Science 2001;10:1470-3.
[36] Laskowski RA, MacArthur MW, Moss DS, Thornton JM. PROCHECK: a program to check the stereochemical quality of protein structures. Journal of Applied Crystallography 1993;26:283-91.

[37] Morris AL, MacArthur MW, Hutchinson EG, Thornton JM. Stereochemical quality of protein structure coordinates. Proteins 1992;12:345-64.
[38] Ramachandran GN, Ramakrishnan C, Sasisekharan V. Stereochemistry of polypeptide chain configurations. Journal of Molecular Biology 1963;7:95-9.
[39] Morris GM, Goodsell DS, Halliday RS, Huey R, Hart WE, Belew RK, et al. Automated Docking Using a Lamarckian Genetic Algorithm and and Empirical Binding Free Energy Function. Journal of Computational Chemistry 1998;19:1639-62.
[40] Kashparov IA, Semisotnov GV, Alakhov Iu B. [Properties and role of tryptophan residues in the polypeptide chain of elongation factor G from *E. coli*]. Biokhimiia 1981;46:1488-98.
[41] Shukla S, Rai V, Banerjee D, Prasad R. Characterization of Cdr1p, a major multidrug efflux protein of *Candida albicans*: purified protein is amenable to intrinsic fluorescence analysis. Biochemistry 2006;45:2425-35.
[42] Martemyanov KA, Gudkov AT. Domain III of elongation factor G from *Thermus thermophilus* is essential for induction of GTP hydrolysis on the ribosome. Journal of Biological Chemistry 2000;275:35820-4.
[43] Bodley JW, Zieve FJ, Lin L, Zieve ST. Formation of the ribosome-G factor-GDP complex in the presence of fusidic acid. Biochemical and Biophysical Research Communications 1969;37:437-43.
[44] Cameron DM, Thompson J, March PE, Dahlberg AE. Initiation factor IF2, thiostrepton and micrococcin prevent the binding of elongation factor G to the *Escherichia coli* ribosome. Journal of Molecular Biology 2002;319:27-35.
[45] Aminake MN, Schoof S, Sologub L, Leubner M, Kirschner M, Arndt HD, et al. Thiostrepton and derivatives exhibit antimalarial and gametocytocidal activity by dually targeting parasite proteasome and apicoplast. Antimicrobial Agents and Chemotherapy 2011;55:1338-48.
[46] Johanson U, Aevarsson A, Liljas A, Hughes D. The dynamic structure of EF-G studied by fusidic acid resistance and internal revertants. Journal of Molecular Biology 1996;258:420-32.
[47] Chen Y, Koripella RK, Sanyal S, Selmer M. *Staphylococcus aureus* elongation factor G--structure and analysis of a target for fusidic acid. FEBS Journal 2010;277:3789-803.
[48] Koripella RK, Chen Y, Peisker K, Koh CS, Selmer M, Sanyal S. Mechanism of elongation factor-G-mediated fusidic acid resistance and fitness compensation in *Staphylococcus aureus*. Journal of Biological Chemistry 2012;287:30257-67.
[49] Okura A, Kinoshita T, Tanaka N. Complex formation of fusidic acid with G factor, ribosome and guanosine nucleotide. Biochemical and Biophysical Research Communications 1970;41:1545-50.
[50] Seo HS, Kiel M, Pan D, Raj VS, Kaji A, Cooperman BS. Kinetics and thermodynamics of RRF, EF-G, and thiostrepton interaction on the *Escherichia coli* ribosome. Biochemistry 2004;43:12728-40.
[51] Savelsbergh A, Rodnina MV, Wintermeyer W. Distinct functions of elongation factor G in ribosome recycling and translocation. RNA 2009;15:772-80.
[52] Seo HS, Abedin S, Kamp D, Wilson DN, Nierhaus KH, Cooperman BS. EF-G-dependent GTPase on the ribosome. conformational change and fusidic acid inhibition. Biochemistry 2006;45:2504-14.
[53] Rodnina MV, Savelsbergh A, Matassova NB, Katunin VI, Semenkov YP, Wintermeyer W. Thiostrepton inhibits the turnover but not the GTPase of elongation factor G on the ribosome. Proceedings of the National Academy of Sciences USA 1999;96:9586-90.

[54] Walter JD, Hunter M, Cobb M, Traeger G, Spiegel PC. Thiostrepton inhibits stable 70S ribosome binding and ribosome-dependent GTPase activation of elongation factor G and elongation factor 4. Nucleic Acids Research 2012;40:360-70.
[55] Tarr SJ, Nisbet RE, Howe CJ. Transcript-level responses of *Plasmodium falciparum* to thiostrepton. Molecular and Biochemical Parasitology 2011;179:37-41.
[56] McConkey GA, Rogers MJ, McCutchan TF. Inhibition of *Plasmodium falciparum* protein synthesis. Targeting the plastid-like organelle with thiostrepton. Journal of Biological Chemistry 1997;272:2046-9.
[57] Johanson U, Hughes D. Fusidic acid-resistant mutants define three regions in elongation factor G of *Salmonella typhimurium*. Gene 1994;143:55-9.
[58] Nagaev I, Bjorkman J, Andersson DI, Hughes D. Biological cost and compensatory evolution in fusidic acid-resistant *Staphylococcus aureus*. Molecular Microbiology 2001;40:433-9.
[59] Norstrom T, Lannergard J, Hughes D. Genetic and phenotypic identification of fusidic acid-resistant mutants with the small-colony-variant phenotype in *Staphylococcus aureus*. Antimicrobial Agents and Chemotherapy 2007;51:4438-46.
[60] Ticu C, Murataliev M, Nechifor R, Wilson KS. A central interdomain protein joint in elongation factor G regulates antibiotic sensitivity, GTP hydrolysis, and ribosome translocation. Journal of Biological Chemistry 2011;286:21697-705.
[61] Ishida T, Kinoshita K. PrDOS: prediction of disordered protein regions from amino acid sequence. Nucleic Acids Research 2007;35:W460-4.
[62] Bhargava K, Templeton P, Spremulli LL. Expression and characterization of isoform 1 of human mitochondrial elongation factor G. Protein Expression and Purification 2004;37:368-76.